

## Study on grain growth and conduction mechanism of spinel nickel ferrite ceramics

Baogang Liu\*, Min Tang, Xiang Wei and Hongjuan Li

School of Energy and Electromechanical Engineering, Hunan University of Humanities, Science and Technology, Loudi 417000, China

The important base of its application performance can be constituted by combining microstructure with electrical conductivity of spinel nickel ferrite ceramics. In this study, nickel ferrite ceramic powders were prepared by a high temperature solid-phase reaction and ceramic blocks were prepared by molding and sintering technology. X-ray diffraction, scanning electron microscopy, conductivity measurement and X-ray photoelectron spectrometry were employed for analyzing the phase composition, microstructure, electrical conductivity, and valence states of Fe ions. The grain growth mode and conduction mechanism of nickel ferrite ceramics were also discussed. Hexagonal growth spirals and growth hillocks were observed on each crystal plane of nickel ferrite single crystals. The growth of nickel ferrite crystals takes place by a spiral dislocation growth mechanism, indicating that the more  $\text{Fe}^{2+}$  ion formed in the sites of octahedral B of  $\text{NiFe}_2\text{O}_4$  ceramics, the better the electrical conductivity of this ceramic materials.

**Key words:** Ceramics, Nickel ferrite, Grain growth, Conduction mechanism.

### Introduction

Spinel ferrites, which serve as materials of commercial importance, are attracting years of concentration. Among various spinel ferrites, nickel ferrite is one of the most attractive materials due to its potential applications and interesting physics. Besides, they have been extensively applied in diverse fields such as data storage [1], catalysts [2], ferrofluids [3], gas sensors [4], magnetic drug delivery [5], antenna material [6] and microwave absorbers [7].

The fundamental understanding of grain growth mode and conduction mechanism of nickel ferrite is of great importance to their applications. In view of this, even after so many years, researchers still show great interest in the grain growth mode and conduction mechanism of nickel ferrite prepared by different techniques. Wang et al. prepared  $\text{NiFe}_2\text{O}_4$  nanoparticles based on differential mean grain sizes by employing a sol-gel auto-combustion method. The disclosure grain growth mechanism oriented with  $\text{NiFe}_2\text{O}_4$  nanoparticles aimed to follow an Ostwald ripening model and grain boundary diffusion model [8]. Šutka et al. applied sol-gel auto combustion for the synthesis of nickel ferrites of p-type with n-type conductivity in virtue of taking control of the relative nickel-iron amounts. In the meanwhile, DC resistivity measurements of room temperature appeared. The grain size did not lead to

dramatic changes in resistivity that p-type nickel ferrite is featured by since the resistivity decreased through four-order magnitude in n-type nickel ferrite [9]. Chavan and other researchers provided the preparation of magnesium - doped nickel ferrite nanoparticles based on auto combustion approach. Moreover, research on the conduction mechanism of ferrites was conducted in virtue of DC resistivity in regards to temperature. According to the attained values of activation energy, the hopping made by small polarons was in charge of the conduction of electrons within nickel ferrite nanoparticles [10]. Nevertheless, to the best of our knowledge, concerning the studies of grain growth mode, up to the present, no detailed discussion has been made on the effect of the amount of  $\text{Fe}^{2+}$  ion on DC electrical conductivity of nickel ferrite.

In the present study, preparations on samples of  $\text{NiFe}_2\text{O}_4$  were implemented on the condition of 1300 °C through solid state reaction. Researches were made on the grain growth mode and the effect exerted by the  $\text{Fe}^{2+}$  ion amounts in octahedral sites upon DC electrical conductivity of nickel ferrite, respectively. Moreover, the above-mentioned experiments were expected to provide information for understanding physical properties of spinel nickel ferrite.

### Experimental

Synthesis was made on samples of  $\text{NiFe}_2\text{O}_4$  through solid state reaction. NiO (99%, Jinchuan, China) of high purity and  $\text{Fe}_2\text{O}_3$  (99%, Qidong, China) with high purity were adopted for functioning the duty of raw materials with ball-milled in the distilled water and

\*Corresponding author:  
Tel : +86-738-8326910  
Fax: +86-738-8326910  
E-mail: liudd2016@126.com

ZrO<sub>2</sub> milling media, which lasted 3 hours. Additionally, 12-hour drought on the condition of 90 °C. Then, calcinations were made on the condition of 1200 °C, which lasted 6 hours in air. Subsequently, the compacts on the calcined powders were made in a uniaxial way on the condition of 50 MPa for the purpose of forming cylindrical blocks (around the diameter of 20 mm and the thickness of 40 mm). Afterwards, the sintering was made on the condition of 1300 °C, which lasted 6 hours in air and nitrogen atmospheres separately. Next, 0.2 degrees Celsius every minute was the condition of the fired samples and the following cooling in order to avoid cracking due to thermal shock.

With X-ray diffraction, examination was made on the phases existing the samples (Rigaku D-max/2550VB+, Tokyo, Japan) on the condition of 40 KV and 250 mA based on Cu-K $\alpha$  radiation. Using scanning electron microscopy, investigations on the microstructure were conducted (JEOL JSM-6360LV, Tokyo, Japan). The valence states of Fe ions were investigated by X-ray photoelectron spectroscopy (VG Multilab 2000, Thermo Electron Corporation, USA). Measurement on DC electrical conductivities was implemented at normal temperature by employing the probe approach of four points.

## Results and Discussion

### X-ray Diffraction Analysis

Fig. 1 illustrates the X-ray diffraction pattern in which NiFe<sub>2</sub>O<sub>4</sub> powders calcined are characterized by at 1200 °C for 6 hours in air. The samples revealed polycrystalline phases situated by a typical cubic spinel structure without any signature of secondary phase. Moreover, the result stemmed out of X-ray diffraction conformed to the JCPDS Card (No. 54-0964). Calculation on the lattice constant was conducted through performing the analysis on the XRD pattern.

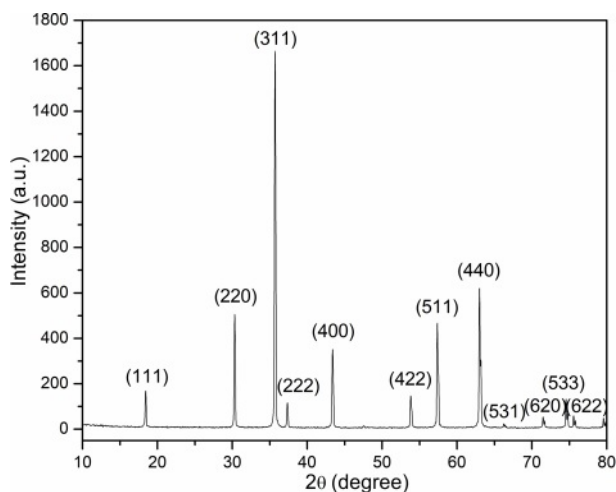


**Fig. 1.** X-ray diffractogram of NiFe<sub>2</sub>O<sub>4</sub> powders calcined at 1200 °C for 6 hours in air.

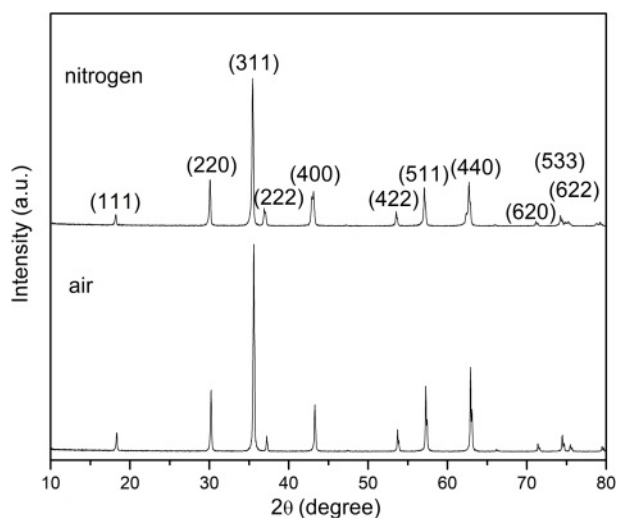


**Fig. 2.** X-ray diffractogram of NiFe<sub>2</sub>O<sub>4</sub> samples sintered at 1300 °C.

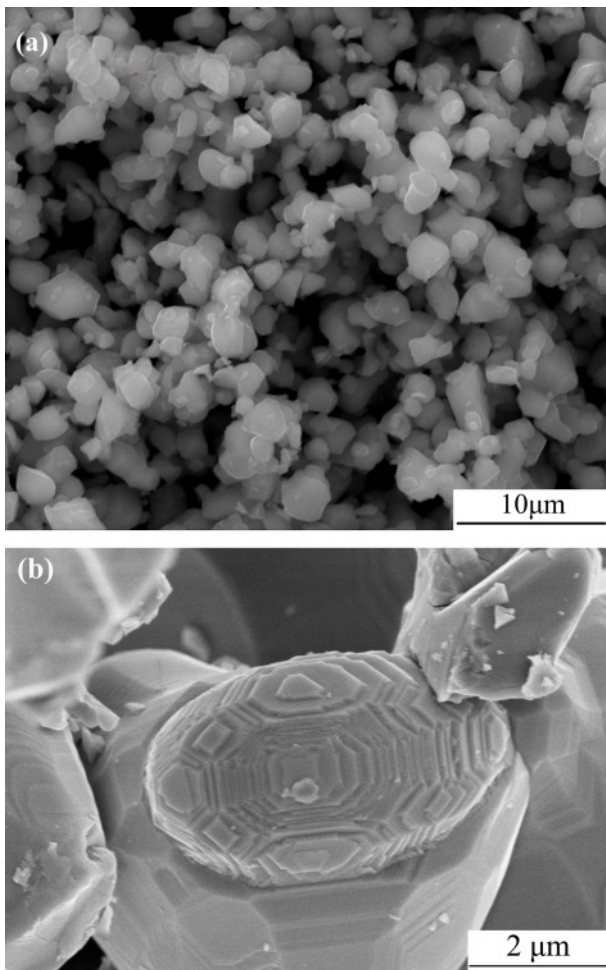
The lattice constant was 8.342 Å, which was almost in consistence with the results reported in the literature [11-13].

Fig. 2 shows the X-ray diffraction patterns of the samples sintered in air and nitrogen atmospheres, separately. The two samples expressed polycrystalline phases presenting a representative cubic spinel structure, indicating that there exists no phase transition during the sintering process.

### Distinct grain growth phenomena

Fig. 3a demonstrates the scanning electron micrograph of NiFe<sub>2</sub>O<sub>4</sub> particles calcined on the in-air condition of 1200 °C for 6 hours. Those ferrite particles featured by an average 1.5 μm grain size displayed a uniform nature and some agglomeration level.

Fig. 3b expresses the scanning electron micrograph that a single-crystal nickel ferrite is featured. Hexagonal growth spirals and growth hillocks were observed on each crystal plane of nickel ferrite single crystals. It also marked the first announced instance where direct visual evidence of grain growth has been obtained on the individual crystal plane of nickel ferrite single crystals prepared by solid state reaction. Crystal growth is frequently dominated by the presence of screw dislocations on the crystal surfaces. Burton, Cabrera and Frank were the introducers of those classical models structured by the evolved vicinal surface [14]. Based on the observation of the kink sites at the facial steps, in this place, exchanges occur among the adatom layer on not only the terraces but also the solid phase. An exposed edge will be shaped wherever a screw dislocation ends up with a crystal face. During the period of growth, it will be of persistence by developing in the form of a 'Growth Spiral' which is oriented with dislocation. Initially, these growing spirals made a least number of turns. Then, they



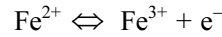
**Fig. 3.** SEM images of  $\text{NiFe}_2\text{O}_4$  powders calcined at  $1200^\circ\text{C}$  for 6 hours at different multiples: (a)  $\times 10000$ ; (b)  $\times 25000$ .

formed hexagonal shapes through the crystal-based hexagonal outline. The above obtained results provide convincing evidence that the growth of nickel ferrite crystals takes place by a spiral dislocation growth mechanism.

### Conduction mechanism

Electrical conductivity can reflect the transporting capability which ion and electron are characterized by in a certain material [15]. Nickel ferrite ceramics serve as transition metal oxide semiconductors featuring the spinel structure and they boast low-mobility materials. It is considered that the above-mentioned transport properties could be derived out of charge transfer among those octahedral cations which was realized through the hopping made by localized d electrons. Furthermore, the electrical conductivity in ferrites could be expounded in the name of the Verwey-de Boer mechanism where electron exchanges among the ions of the same element existing within the valence state [16]. These ions exist in a random distribution over crystallographically equivalent lattice sites. Nickel ferrite, the electronic hopping occurring among  $\text{Fe}^{2+}$

and  $\text{Fe}^{3+}$  ions at octahedral sites, boasts one of the major systems allowing electrical transport [17], which could be interpreted with the electron exchanging processes as follows:



Based on the four-point probe approach, measurement was conducted to the direct current conductivities in which the samples are featured by at normal temperature. According to the results, the direct current conductivities that the samples were sintered in air were  $4.11 \times 10^{-3} \text{ S/cm}$ , and  $5.48 \times 10^{-1} \text{ S/cm}$ , representing the value of the samples sintered in nitrogen. Obviously, the direct current conductivities which the samples sintered in nitrogen are featured by expressing a dramatic enhancement compared with that in-air sintered. These electrical conductivities embraced the difference from the oxygen partial pressure on the condition of sintering. Our experiment contains the synthesis of the whole nickel ferrite powders oriented with well-prepared samples in air. Initially, before sintering the above samples, the oxygen ion vacancy's concentration in those powders presented the value in

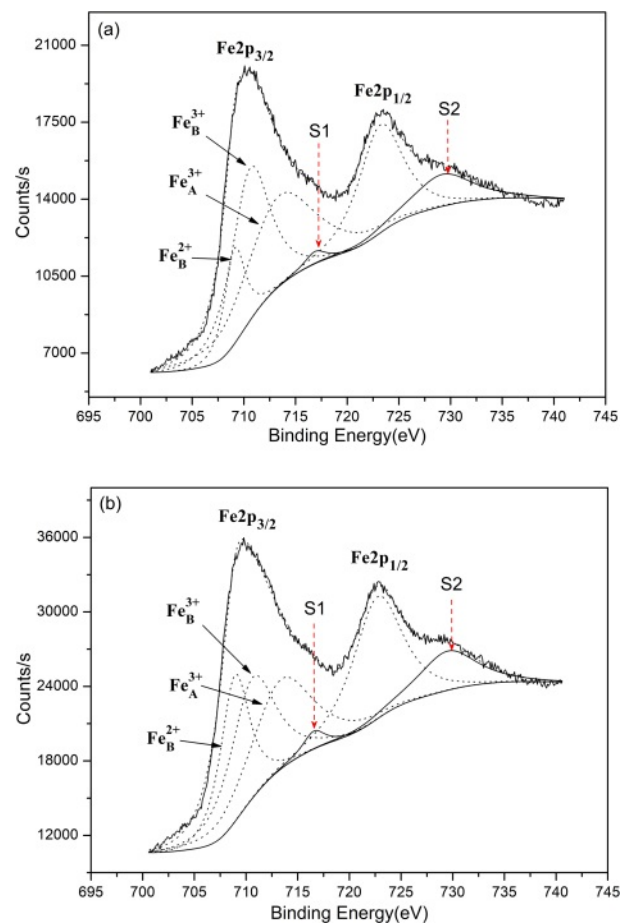


**Fig. 4.** XPS spectra of the samples sintered at  $1300^\circ\text{C}$ : (a) sintered in air; (b) sintered in nitrogen;  $\text{Fe}^{3+}_A$  tetrahedral A-site;  $\text{Fe}^{3+}_B$  octahedral B-site;  $\text{Fe}^{2+}_B$  octahedral B-site; S1 and S2 satellite peaks.

**Table 1.** Relative values of Fe2p peaks for NiFe<sub>2</sub>O<sub>4</sub> samples sintered in air and nitrogen at 1300 °C.

Sintering atmosphere	Peak position (eV)			Peak area (eV/s)			Fe <sup>2+</sup> <sub>B</sub> /Fe <sup>3+</sup> <sub>B</sub> (%)
	Fe <sup>2+</sup> <sub>B</sub>	Fe <sup>3+</sup> <sub>B</sub>	Fe <sup>3+</sup> <sub>A</sub>	Fe <sup>2+</sup> <sub>B</sub>	Fe <sup>3+</sup> <sub>B</sub>	Fe <sup>3+</sup> <sub>A</sub>	
air	709.1	710.6	713.4	12207	37127	41545	24.7
nitrogen	708.9	710.6	713.4	46770	59302	59525	44.1

equilibrium with air. As a result, as the samples pressing in cylindrical blocks went into the atmosphere of in-air sinter and nitrogen, the gas phase was where the oxygen ions aimed to massively transfer with these oxygen molecules. Considering the much lower oxygen partial pressure on the nitrogen atmosphere compared with the in-air pressure, some lattice oxygen would be released out of the oxides as the samples were sintered in nitrogen atmosphere for forming the oxygen vacancy. Therefore, lower valence was the result of some portion of Fe<sup>3+</sup> ions (Fe<sup>3+</sup> → Fe<sup>2+</sup>) for maintaining the charge neutrality of lattice. These formed Fe<sup>2+</sup> ions were strongly inclined to gain the location of the octahedral B-site [18]. The enhancing Fe<sup>2+</sup> ion concentration located in the octahedral sites contributed to the enhancement of those electrons' hopping rate, thus producing a more powerful electrical conductivity. By contrast, the concentration of oxygen ion vacancy featured by the in-air samples sintered represented the equal value to air. To further confirm the validity of our analysis, in virtue of X-ray photoelectron spectroscopy, examination was conducted on the Fe ions' valence states and the Fe<sup>2+</sup> ion concentration that the octahedral B-sites harbored. Fig. 4 demonstrate the XPS spectra of the samples sintered in air and nitrogen. Tabulation and calculation were made to the relative values in Table 1. It can be found that both Fe<sup>3+</sup> ion and Fe<sup>2+</sup> ion present in the two samples. The atomic rate of Fe<sup>2+</sup><sub>B</sub>/Fe<sup>3+</sup><sub>B</sub> for the samples sintered in nitrogen atmosphere had a dramatic enhancement when compared with in-air samples. Thus, it can be concluded that the more the Fe<sup>2+</sup> ion amounts which was formed in the octahedral B sites of NiFe<sub>2</sub>O<sub>4</sub> ceramics, the better the electrical conductivity of this ceramic materials.

### Conclusion

To conclude, nickel ferrite ceramic powders were prepared by a high temperature solid-phase reaction and ceramic blocks were prepared by molding and sintering technology. Hexagonal growth spirals and growth hillocks prove that the growth of nickel ferrite crystals takes place by a spiral dislocation growth mechanism. It indicates that the more the amount of

Fe<sup>2+</sup> ion formed at octahedral B sites of NiFe<sub>2</sub>O<sub>4</sub> ceramics, the better the electrical conductivity of this ceramic materials.

### Acknowledgements

The current work was in the support of the Scientific Research Fund of Hunan Provincial Education Department (18C0878) and the Hunan Provincial Natural Science Foundation of China (2020JJ6094).

### References

1. V. Kumari, K. Dey, S. Giri, A. Bhaumik, RSC. Adv. 6 (2016) 45701.
2. H. Jian, Y. Song, A. Riisager, Catal. Sci. Technol. 8 (2018) 790.
3. P.B. Kharat, S.D. More, S.B. Somvanshi, K.M. Jadhav, J. Mater. Sci: Mater. Electron. 30 (2019) 6564.
4. J. Niresh, N. Archana, S. Neelakrishnan, V.M. Sivakumar, D.S. Dharun, J. Ceram. Process. Res. 21 (2020) 343.
5. K.S. Joshy, R. Augustine, A. Mayeen, A. Susan M, A. Hasan, S. Thomas, H. Chi, New. J. Chem. 44 (2020) 18162.
6. I. Silva, A.G. Assuno, J. Oliveira, J. Guerra, M. Sousa, Microw. Opt. Technol. Lett. 62 (2020) 2895.
7. S. Pawar, M. Gandi, I. Arief, B. Krause, P. Pötschke, S. Bose, Chemistry. Select. 2 (2017) 5984.
8. Y. Wang, L. Li, Y. Zhang, X. Chen, S. Fang, G. Li, J. Phys. Chem. C 121 (2017) 19467.
9. A. Šutka, R. Pärna, T. Käämbre, V. Kisand, Physica B 456 (2015) 232.
10. P. Chavan, L. R. Naik, Phys. Status Solidi A 214 (2017) 170077.
11. S. Debnath, R. Das, J. Alloys Compd. 852 (2021) 156884.
12. M. Khan, S. Bisen, J. Shukla, A. Mishra, P. Sharma, J. Supercond. Nov. Magn. 34 (2021) 763.
13. T. Vigneswaria, P. Rajib, J. Ceram. Process. Res. 17 (2016) 999.
14. W.K. Burton, N. Cabrera, F.C. Frank, Phil. Trans. Roy. Soc. London, Ser. A 243 (1951) 299.
15. B. Liu, K. Zhou, Z. Li, D. Zhang, L. Zhang, Mater. Res. Bull. 45 (2010) 1668.
16. L.G. Van Uitert, J. Chem. Phys. 23 (1955) 1883.
17. V. Baco-Carles, I. Pasquet, V. Laurent, A. Gabriel, P. Tailhades, Solid. State. Sci. 11 (2009) 1503.
18. M. Bhagavantha Reddy, V. Devender Reddy, P. Venugopal Reddy, Mod. Phys. Lett. B 8 (1994) 959.